Journal of Solid Mechanics Vol. 9, No. 3 (2017) pp. 543-554

Influence of the Vacancies on the Buckling Behavior of a Single–Layered Graphene Nanosheet

S.M.H. Farrash , M. Shariati *, J. Rezaeepazhand

Department of Mechanical Engineering, Faculty of Engineering, Ferdowsi University of Mashhad, Mashhad, Iran

Received 11 June 2017; accepted 12 August 2017

ABSTRACT

Graphene is a new class of two-dimensional carbon nanostructure, which holds great promise for the vast applications in many technological fields. It would be one of the prominent new materials for the next generation nano-electronic devices. In this paper the influence of various vacancy defects on the critical buckling load of a single-layered graphene nanosheet is investigated. The nanosheet is modeled on the base of structural mechanics approach which covalent bonds between atoms are modeled as equivalent beam elements in a finite element model. The mechanical properties of the nanosheet extracted from the model are in good agreement with those of other research works. Effect of the number of vacancies and their positions on the critical buckling load is investigated in the present work. Our results show that the location of the vacancy has a significant role in the amount of critical buckling load. Furthermore, as the density of the vacancies increases, the value of critical buckling load decreases and the relationship is approximately linear.

Keywords: Graphene; Structural mechanics; Buckling; Vacancy defect**.**

1 INTRODUCTION

AFTER the discovery of carbon nanotubes, efforts have been made to study the nano size graphene sheets. Analysis of graphene sheets is a fundamental issue in the study of the nanomaterials since many of the carbon-based nanostructures for example, carbon nanotubes, fullerenes, nanorings etc. are viewed as deformed graphene sheets. Graphene is a new class of two- dimensional carbon nanostructure, which holds great promise for the vast applications in many technological fields. It would be one of the prominent new materials for the next generation nano- electronic devices. Reports related to its applications as strain sensor [1], mass and pressure sensors [2], atomic dust detectors [3], enhancer of surface image resolution [4] are observed [5]. In particular, graphene sheets are the thinnest material known to the current science [6]. A monolayer of carbon atoms tightly packed into a two-dimensional hexagonal lattice makes up a single layer graphene sheet (SLGS), which is the basic building block for bulk graphite and carbon nanotubes (CNTs) [7].

To analyze mechanical behavior of graphene, two numerical tools are available. Molecular dynamics simulation is a technique that allows one to determining the physical and mechanical properties of materials in nanoscale. This achieved by solving Newton's equations of motion with the atoms interacting through assumed interatomistic potentials [8, 9,10]. The second method which is known as structural mechanic approach is based on finite element

*Corresponding author. Tel.: +98 513 880 5159; Fax: +98 513 880 6055.
E-mail address: mshariati44@um.ac.ir (M.Shariati).

models. The inter-atomic interactions due to covalent and non-covalent bonds are replaced by beam and spring elements, respectively in the structural model.

The structural mechanics approach developed by Li and Chou [11]. This model considers a single-walled carbon nanotube as a geometrical frame-like structure so that primary bonds between atoms act as loadbearing beam members, while the carbon atoms are seen as joints of these members. By linking structural mechanics and molecular mechanics, they have obtained the sectional property parameters of these beam members. Study of the elastic properties of single-walled carbon nanotubes containing vacancy defects using nanoscale continuum modeling implemented with beam elements was presented by Sakharova et al. [12]. Since the structural mechanics approach is an established technique in nanotube applications, it is the logical choice for the mechanical analysis of the graphene sheet as well [13].

Hemmasizadeh et al. [14] proposed an equivalent continuum model for studying the mechanical behavior of single-layered graphene sheets. By combining continuum and atomistic approaches, Lu and Huang [7] investigate the mechanical properties of single-atomic-layer graphene sheets. Shokrieh et al. [15] presented an analytical formulation to predict the elastic moduli of graphene sheets and carbon nanotubes using a linkage between lattice molecular structure and equivalent discrete frame structure. Cheng and shi [16] predicted equivalent mechanical properties of monolayer graphene sheets by an improved molecular structural mechanics model.

A defect which occurs as a vacancy within the hexagonal network may decrease the mechanical properties of nano sheet and could downgrade its capability as a mechanical reinforcement. Several authors have studied the effect of defects and vacancies on graphene sheets properties from the atomistic point of view, although the focus has been mostly on the electronic properties [17–20]. The fracture behavior of a graphene sheet, containing a center crack was characterized based on the atomistic simulation and the concept of continuum mechanics [21]. An atomistic based finite bond element model has been developed to study the effects of multiple Stone–Wales defects on mechanical properties of graphene sheets and carbon nanotubes [22]. The influence of vacancies on the elastic properties of a single-layer graphene sheet is investigated using atomistic finite element analysis by Tapia et al. [6]. Canadija et al. [13] represented the influence of the vacancy location and the density of vacancies on the bending behavior of a SLGS.

When compressive loads are applied to the plate, it tends to buckle. Understanding the buckling behavior of plates is an important issue from design perspective. Graphene sheets as an upcoming nano engineering structures can also be subjected to in-plane loads. For proper use of graphene sheets as microelectromechanical system (MEMS) and nanoelectromechanical system (NEMS) components, its stability response under in-plane load should be studied. Thus there is a strong encouragement for acquiring proper understanding and mathematical modeling of the buckling of graphene sheets. Though study of buckling of graphene sheets is an important factor for proper design of nanodevices, miniscule numbers of studies are reported. [5].

In this study, the influence of various vacancy defects on the critical buckling load of a single-layered graphene nanosheet is investigated. The nanosheet is modeled on the base of structural mechanics approach using Abaqus software.

2 STRUCTURAL MECHANICS APPROACH TO MODELCARBON NANOSHEETS

We have proposed a structural mechanics method to model the SLGS. The total steric potential energy due to interactions between carbon atoms can be represented by [13]

$$U_{total} = \sum U_r + \sum U_\theta + \sum U_\varphi + \sum U_\omega + \sum U_{vdw} \tag{1}$$

where U_r is for a bond stretch interaction, U_θ for a bond angle bending, U_φ for a dihedral angle torsion, U_ω for an improper (out-of-plane) torsion, U_{vdw} for a nonbonded van der Waals interaction, as shown in Fig. 1. In general, for covalent systems, the main contributions to the total steric energy come from the first four terms, which have included four-body potentials. Under the assumption of small deformation, the harmonic approximation is adequate for describing the energy [23]. For sake of simplicity and convenience, we adopt the simplest harmonic forms and merge the dihedral angle torsion and the improper torsion into a single equivalent term, i.e.

$$U_r = \frac{1}{2} k_r (r - r_0)^2 = \frac{1}{2} k_r (\Delta r)^2 \tag{2}$$

$$U_\theta = \frac{1}{2}k_\theta(\theta-\theta_0)^2 = \frac{1}{2}k_\theta(\Delta\theta)^2 \tag{3}$$

$$U_\tau = U_\varphi + U_\omega = \frac{1}{2}k_\varphi(\Delta\varphi)^2 \tag{4}$$

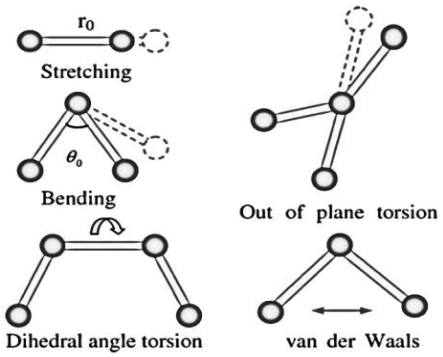

Fig. 1
Interatomic interactions in molecular mechanics [13].

where k_r, k_θ and k_φ are the bond stretching force, bond angle bending force and torsional resistance constant, respectively. The symbols Δr, $\Delta\theta$ and $\Delta\varphi$ represent the bond stretching increment, the bond angle change and the angle change of bond twisting, respectively.

In a carbon nanosheet, the carbon atoms are bonded to each other by covalent bonds and form hexagons on the wall of the tube. These covalent bonds have their characteristic bond lengths and bond angles in a three-dimensional space. When a nanosheet is subjected to external forces, the displacements of individual atoms are constrained by these bonds. The total deformation of the nanosheet is the result of these bond interactions. By considering the covalent bonds as connecting elements between carbon atoms, a nanosheet could be simulated as a frame-like structure. The carbon atoms act as joints of the connecting elements.

In the following, we establish the relations between the sectional stiffness parameters in structural mechanics and the force constants in molecular mechanics. For convenience, we assume that the sections of carbon–carbon bonds are identical and uniformly round. Thus it can be assumed that *Ix* = *Iy* = *I* and only three stiffness parameters, *EA*, *EI* and *GJ*, need to be determined. Because the deformation of a space frame results in the changes of strain energies, we determine the three stiffness parameters based on the energy equivalence. Notice that each of the energy terms in molecular mechanics (Eqs. (2) – (4)) represents an individual interaction and no cross-interactions are included, hence we also need to consider the strain energies of structural elements under individual forces. According to the theory of classical structural mechanics, the strain energy of a uniform beam of length *L* subjected to pure axial force *P* (Fig. 2(a)) is

$$U_P = \int_0^L \frac{P^2}{2EA}dL = \frac{EA}{2L}(\Delta L)^2 \tag{5}$$

where ΔL is the axial stretching deformation. The strain energy of a uniform beam under pure bending moment *M* (Fig. 2(b)) is

$$U_M = \int_0^L \frac{M^2}{2EI}dL = \frac{EI}{2L}(2\alpha)^2 \tag{6}$$

where α denotes the rotational angle at the ends of the beam. The strain energy of a uniform beam under pure torsion *T* (Fig. 2(c)) is

$$U_T = \int_0^L \frac{T^2}{2GJ} dL = \frac{GJ}{2L}(\Delta\beta)^2 \tag{7}$$

where $\Delta\beta$ is the relative rotation between the ends of the beam.

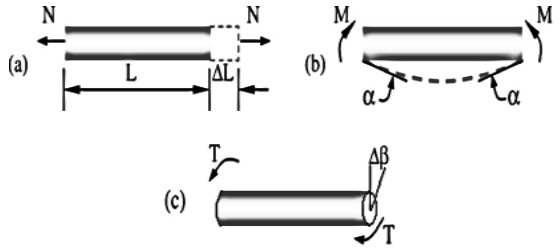

Fig. 2
Pure tension, bending and torsion of an element.

It can be seen that in Eqs. (2) – (7) both U_r and U_P represent the stretching energy, both U_θ and U_M represent the bending energy, and both U_τ and U_T represent the torsional energy. It is reasonable to assume that the rotation angle 2α is equivalent to the total change $\Delta\theta$ of the bond angle, ΔL is equivalent to Δr, and $\Delta\beta$ is equivalent to $\Delta\varphi$. Thus by comparing Eqs. (2) – (4) and Eqs. (5) – (7), a direct relationship between the structural mechanics parameters *EA*, *EI* and *GJ* and the molecular mechanics parameters k_r, k_θ and k_φ are deduced as follows [13]:

$$\frac{EA}{L} = K_r \tag{8}$$

$$\frac{EI}{L} = K_\theta \tag{9}$$

$$\frac{GJ}{L} = K_\varphi \tag{10}$$

where *E* and *G* are the beam elastic and shear moduli, respectively, *A* is the cross-sectional area, *L* the beam length (bond distance between carbon atoms), *I* the moment of inertia and *J* the polar moment of inertia of the beam. Eqs. (8–10) establishes the foundation of applying the theory of structural mechanics to the modeling of carbon nanotubes or other similar fullerene structures. As long as the force constants k_r, k_θ and k_φ are known, the sectional stiffness parameters *EA*, *EI* and *GJ* can be readily obtained.

3 MODELING OF NANOSHEETS USING FINITE ELEMENT MODEL

The structural model discussed above describes a nanosheet model using beam elements. Also, the carbon atoms will be denoted by nodes at appropriate positions. By assuming a circular beam section with diameter *d*, the sectional and material properties of the beam element are determined as follows:

$$d_b = 4\sqrt{\frac{k_\theta}{k_r}}, E = \frac{k_r^2}{4\pi k_\theta}, G = \frac{k_r^2 L k_\varphi}{8\pi k_\theta} \tag{11}$$

The force field constants k_r, k_θ and k_φ are assumed $6.25\times10^{-7}\ N/nm$, $8.76\times10^{-10}\ Nnm/rad^2$ and $2.78\times10^{-10}\ Nnm/rad^2$ respectively. Furthermore, the carbon-carbon bond length *L*=0.142 *nm* is used [24-26].

Substituting these parameters into Eq. (11) we get

$$d_b = 0.147\ nm, E = 5.49\ Tpa, G = 0.87\ Tpa \tag{12}$$

These parameters are used as inputs to the finite element model. To model the atomic bonds, a two node spacial beam element is used in ABAQUS. A zig-zag SLGS of side lengths $a = 6.248\ nm$ and $b = 4.182\ nm$ was modeled. The model is illustrated in Fig. 3. The hexagonal lattice of SLGS and its dimensions are demonstrated in Fig. 3(a). Carbon–carbon bonds are modeled as beam elements and nodes are located at carbon atom positions (Fig. 3(b)).

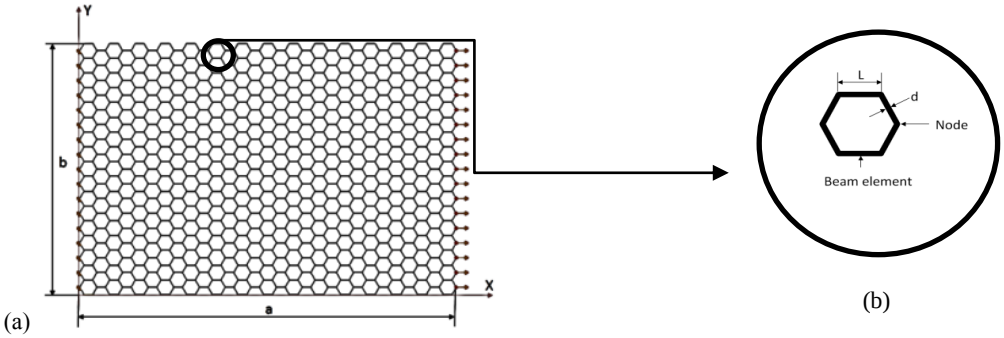

Fig. 3
SLGS., (a) Finite element model, (b) Equivalent beam model.

4 SLGS VACANCY PATTERNS

In present work, the Tapia et al. [6] types of vacancy defects are assumed. Fig. 4 displays the locations and labels of vacancies are selected to provide adequate information about effect of positions and densities of vacancies on buckling response of graphene nanosheet. Analyzed sheets were made up of 29×17 hexagonal rings. A vacancy was simply modeled by the elimination of a corresponding finite element node and three corresponding beam elements used for bonds simulation.

The case ‘‘SLGS’’ represents the baseline case of a graphene sheet without vacancy. Configurations labeled with letters ‘‘C’’, ‘‘U’’, ‘‘L’’, ‘‘B’’ and ‘‘F’’ represent cases with a single vacancy located at the center, upper, lower, back and front part of the sheet, respectively. Configurations ‘‘UX3’’, ‘‘CX3’’ and ‘‘LX3’’ contain three vacancies equally spaced in a row along the *x*-direction, with the three vacancies located at a constant *y* which is different for each configuration. Configurations‘‘BY3’’, ‘‘CY3’’, and ‘‘FY3’’ are analogous to UX3, CX3 and LX3 but the three vacancies are located in a column along the *y*-direction at different *x*-positions for each case. Configurations‘‘CX5’’, ‘‘CX7’’and ‘CX9’’contain five, seven and nine vacancies, respectively, spaced along a central row at *y* = b/2. Finally, configurations ‘‘A5’’, ‘‘A9’’, and‘‘A21’’ are arrays of five, nine and 21 vacancies as shown in Fig. 4.

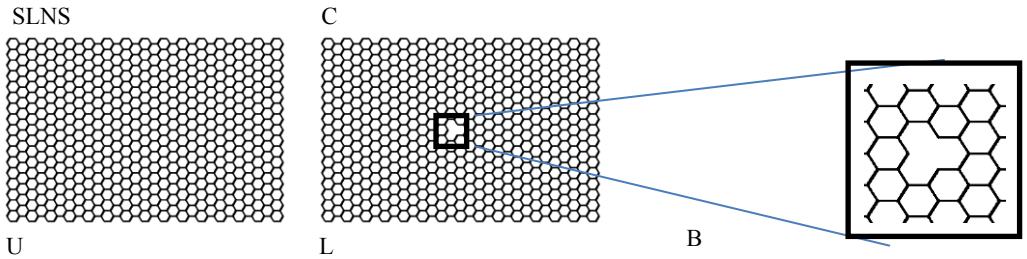

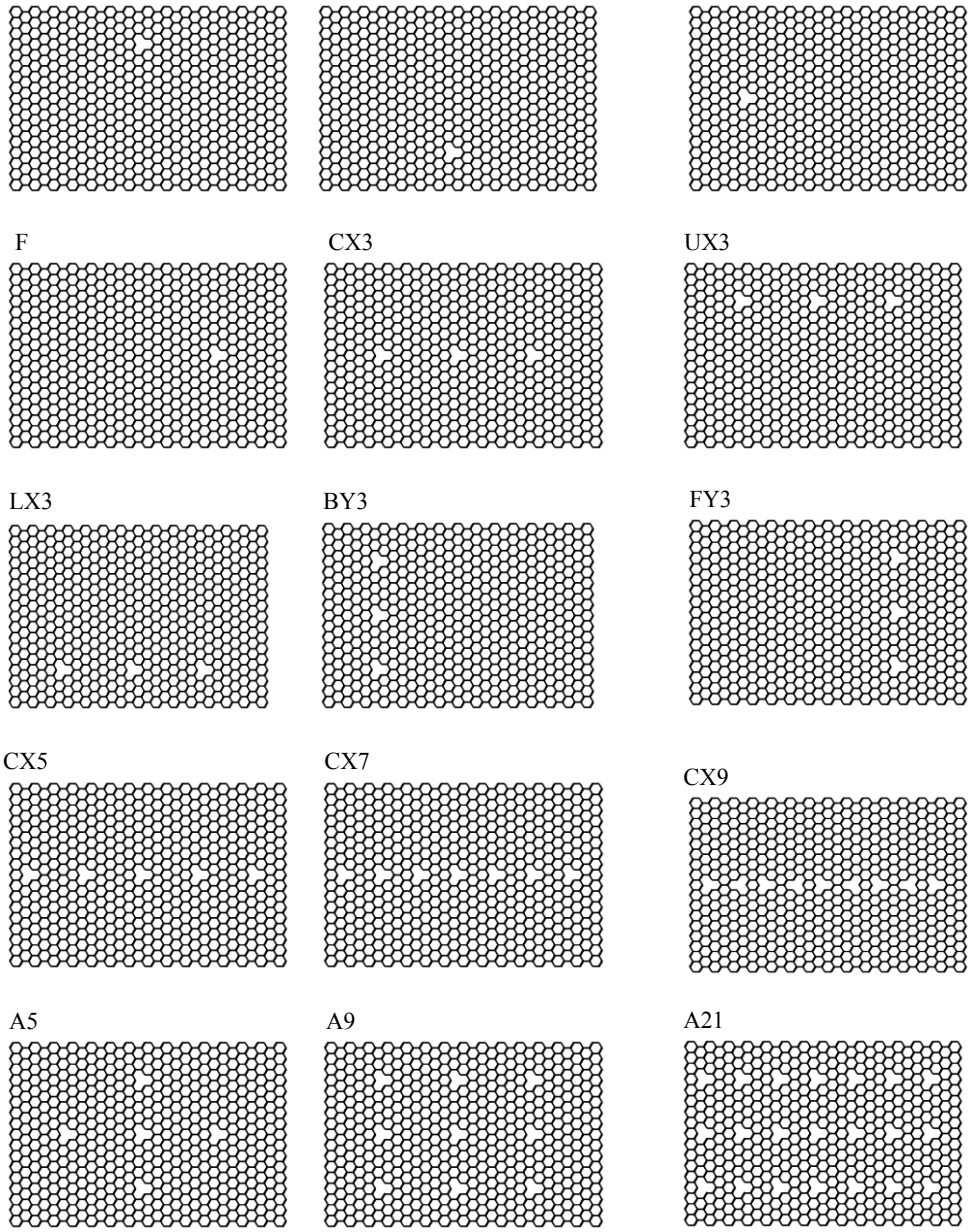

Fig. 4
Graphene sheets – labels and vacancy positions, according to Tapia et al.[6]

5 MODEL VALIDATION

To validate the model, the values of elastic properties of the pristine SLGS, the Young's modulus, shear modulus and poison's ratio have been calculated and compared to those of other researches in Table 1.

The Young's modulus of a material is the ratio of normal stress to normal strain as obtained from a uniaxial tension test. So, the Young's modulus of SLGS (E_0) has been calculated using the following equation:

$$E_0 = \frac{\sigma_x}{\varepsilon_x} = \frac{P/A_0}{\Delta a/a} \tag{13}$$

where P is the axial force, A is the cross sectional area of the nanosheet subjected to axial load, Δa is elongation and a is the initial length of nanosheet. Moreover, A is equal to $b \times t$ where t is the thickness of the nanosheet. The value of the thickness has been assumed 0.34 *nm* [6, 12, 27].

Fig. 5 shows the displacement contour plots in x and y directions. Using Abaqus model, the values of E, G and υ for pristine sheet have been obtained 1.033 *Tpa*, 0.192 *Tpa* and 0.0821 respectively. As it can be seen in Table 1. the obtained Young's modulus of the nanosheet by the present work is almost the same as their comparable results. Furthermore, the values of G and υ are found 0.19 *Tpa* and 0.07 respectively from our simulation which are in good agreement with the values presented by Tapia et al. [6].

To confirm the validation of models with vacancy defects, the simulation of tensile test and shear test were executed for these models and the mechanical properties were compared to those from Tapia et al.[6]. The results for elastic modulus are presented in Fig. 6.

Fig. 6(a) and 6(b) show the values of E/E_0 when the location of the single or triple vacancy defect varies along x and y direction, respectively. Based on these figures, although the Young's modulus reduces by increasing the number of vacancies, the location of vacancies has no significant effect on this value. Fig. 6(c) displays the influence of the number of vacancies on the nanosheet Young's modulus. Considering the graph, we can say that a rise in the number of vacancies brings about an approximately linear decline in the value of the nanosheet Young's modulus.

The effect of the areal density of vacancies (A/A_0, where $A_0 = a \times b$ is the full area of the nanosheet and A is total area of the vacancies) on the elastic properties of the sheet for configurations C, A5, A7, A9 and A21 has been illustrated in Fig. 6(d). A linearly decreasing behavior is observed between E and the areal density of vacancies.

As it can be seen from these graphs, the values of elastic modulus, obtained from our models match well with those predicted by Tapia et al. [6].

Table 1
Comparision of Young's modulus results for single layered graphene sheet (E_0).

Investigators	Young's modulus (*Tpa*)
Present work	1.041
Tapia et all. [6]	1.042
Sakhaee-pour[27]	1.040
Shokrieh and Rafiee [15]	1.04
Li and Chou [12]	1.033
Lier et al. [28]	1.11
Kudin et al.[29]	1.029
Xiao et all. [30]	1.06
Reddy et all. [31]	1.11
Wu et all. [32]	1.06
Natsuki et all. [33]	1.06

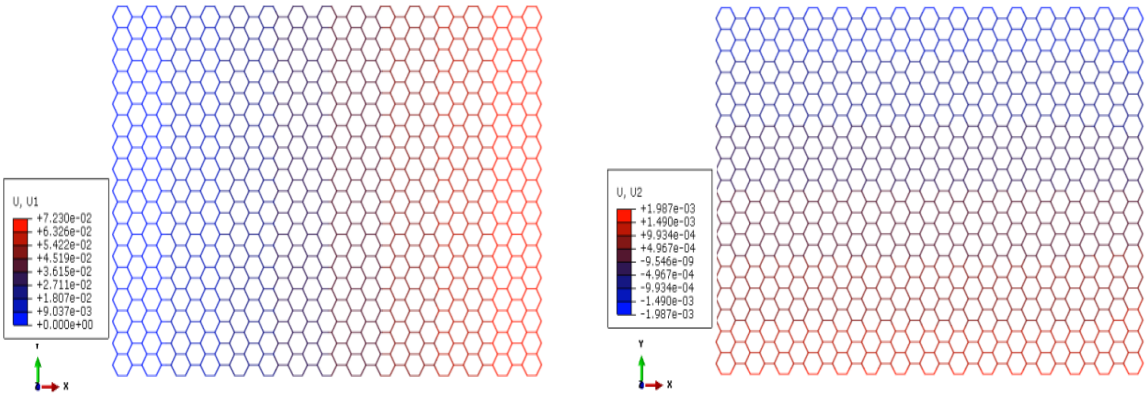

(a) (b)

Fig. 5
Displacement contour plots, (a) x direction, (b) y direction.

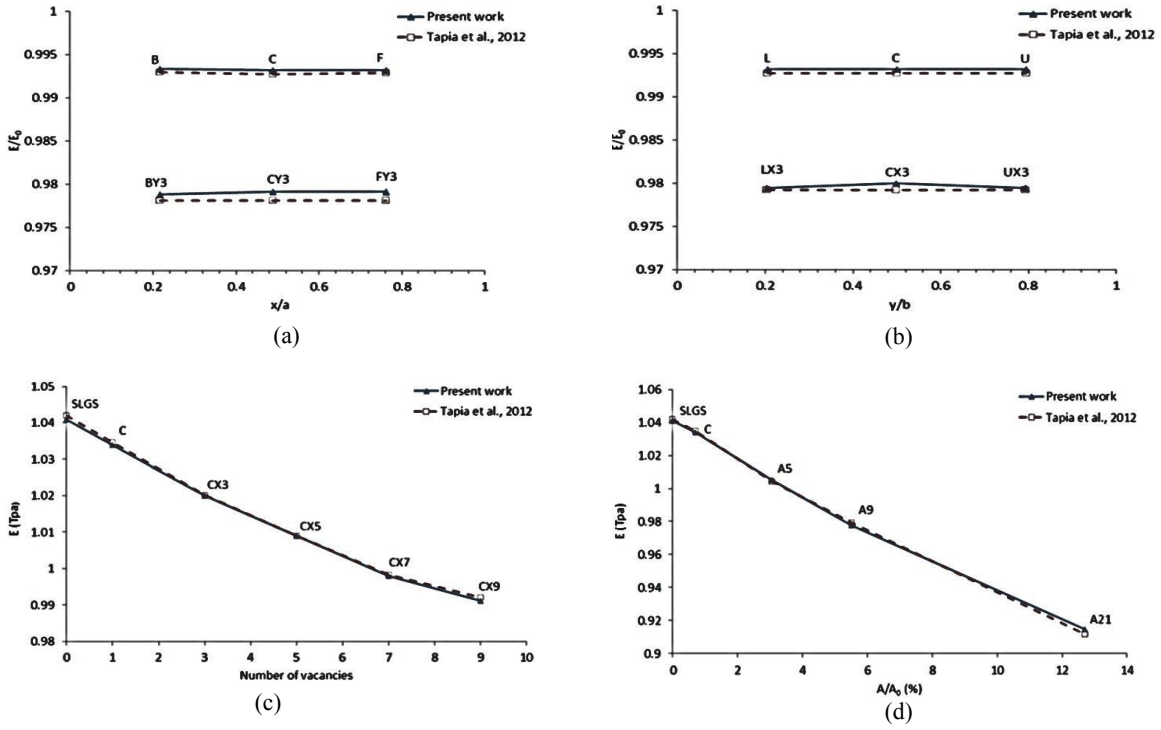

Fig. 6
The influence of location and number of vacancies on the Young's modulus, (a) single or triple vacancy defect varies along *x* direction, (b) single or triple vacancy defect varies along *y* direction, (c) influence of the number of vacancies along *x* direction, (d) the effect of the areal density of vacancies.

6 INFLUENCE OF THE VACANCY DEFECT ON THE BUCKLING BEHAVIOR OF A SLGS

On the base of the lack of study on the buckling of thin nanoplates such as graphene sheets with allowance for vacancy defects, this article presents the influence of the vacancy location and the density of defects on the critical buckling load of a single-layered graphene nanosheet.

The assumed rectangular simply supported SLGS is shown in Fig. 7. A distributed load has been applied on the edge at $x=0$; furthermore, a displacement boundary condition $U_x=0$ has been implemented on all nodes which are located at x=a. Let the magnitude of compressive force per unit length of the edge be denoted by N_x. By gradually increasing N_x we arrive at the condition where the flat form of equilibrium of the compressed plate becomes unstable and buckling occurs.

The elastic buckling load of the model is computed by the structural stability method [34] that finds compressive forces by which the generated model does not have a unique equilibrium configuration. The compressive forces are obtained through the eigenvalue problem solution. Then, the minimum force is considered as the buckling force of the SLGS. In order to study the effect of various defect types on the elastic buckling behavior of the SLGS, various vacancies according to Fig. 4 were generated and corresponding buckling loads are calculated. First buckling mode shapes for some vacancy defects are demonstrated in Fig. 8.

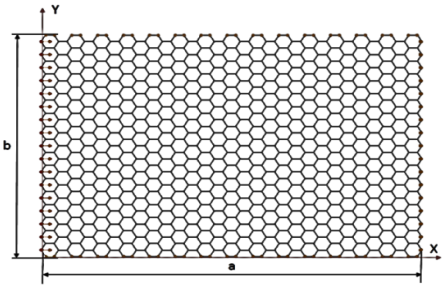

Fig. 7
Simply supported SLGS under in-plane compression load, At $x=0$; $U_z=0$, At $x=a$; $U_x= U_z=0$, At $y=0$; $U_z=0$, At $y=b$; $U_z=0$.

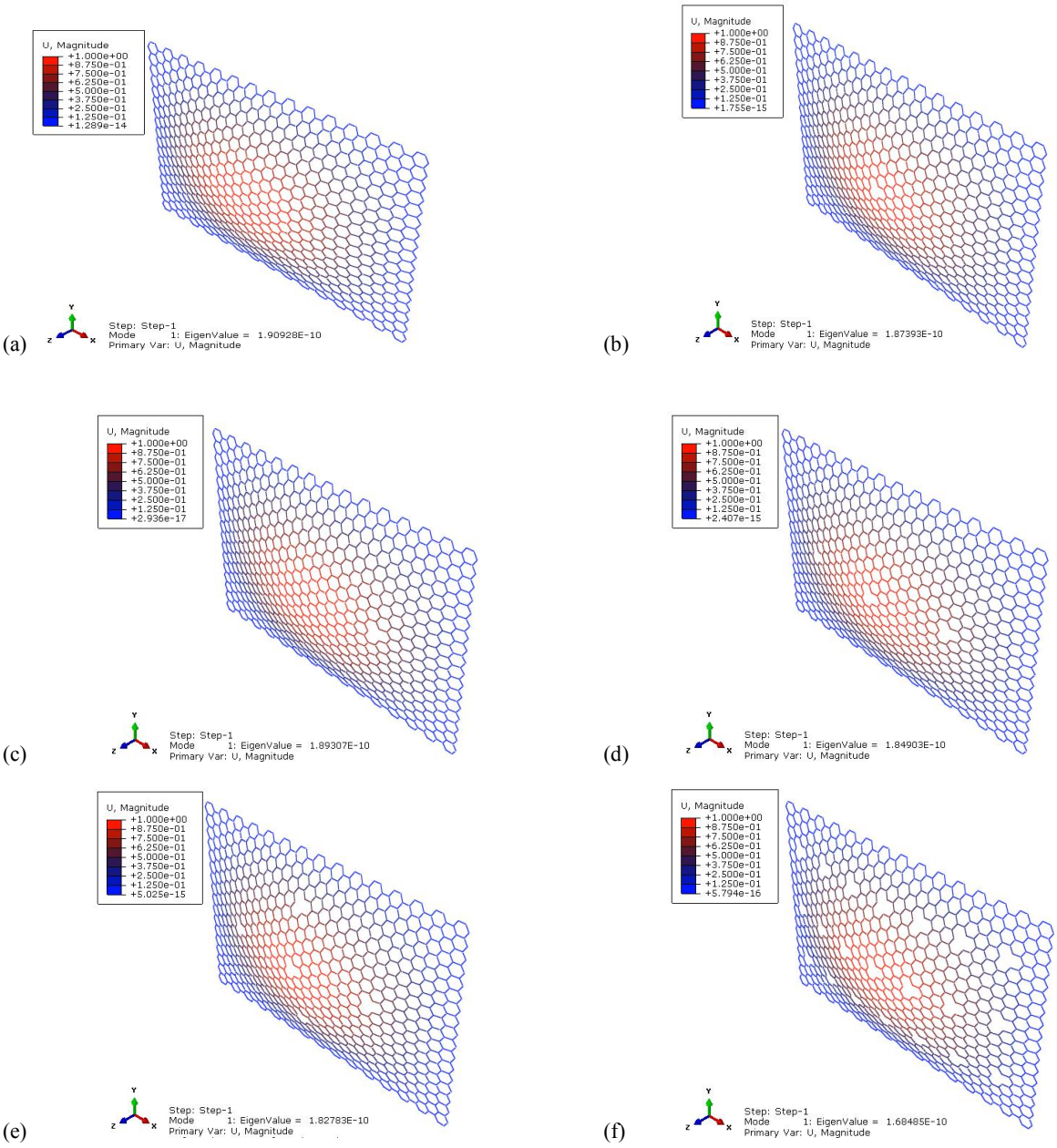

Fig. 8
First buckling mode shape of a single layer graphene nanosheet with different defects, (a) SLGS, (b) "C" defect configuration, (c) "F" defect configuration, (d) "CX3" defect configuration, (e) "A5" defect configuration, (f) "A21" defect configuration.

7 RESULTS

The vacancy position, number of vacancies in one direction and the areal density of the vacancies affect the critical buckling load of the nanosheet. To facilitate the interpretation of the results, all buckling loads calculated for the sheet with vacancies were normalized with the corresponding results of the pristine SLGS that is N_x/N_{xSLGS}. Fig. 9 shows the variation of normalized critical buckling load considering various locations and densities of the defect.

The influence of the vacancy position in horizontal direction has been shown in Fig. 9(a). The horizontal axis (x/a) corresponds to the nondimensional location of the vacancy in B, C and F configurations (see Fig. 4). This line graph indicates that existence of a single vacancy in the back or front of a nanosheet leads to a slight decrease, approximately 0.5 %, in the amount of the N_x/N_{xSLGS} while a central defect develops over 1.5% reduction in this value. Also triple vacancy defects, BY3, CY3 and FY3, reduces the critical buckling load by different percentages. BY3 and FY3 vacancy types result in a decrease of about 1.5 % and CY3 defect causes over than 3% drop in the value of N_x/N_{xSLGS}.

Fig. 9(b) represents the effect of vacancy position when its position changes in vertical direction. The horizontal axis (y/b) is the nondimensional location of the vacancy in L, C and U configurations. Moreover, according to Fig. 4, triple vacancy defects, LX3, CX3 and UX3 indicate the position of a triple vacancy in y direction. Comparison of Fig. 9(a) and Fig. 9(b) demonstrated that the percentages of reduction of the amount of normalized critical buckling loads are similar to those when the vacancy location changes in x direction. In both cases the minimum critical buckling loads are related to central defects (C, CX3, CY3), in which the maximum strain occurs.

The influence of number of vacancies in horizontal direction on the nanosheet critical buckling load is shown in Fig. 9(c). Regarding the graph, the normalized critical buckling load decreases gradually and falls to the lowest point with more than 6% reduction at CX9 configuration.

When there are more vacancies in both horizontal and vertical directions, the areal density of vacancies increases. The influence of the areal density of vacancies on the normalized critical buckling load of the nanosheet is illustrated in Fig. 9(d). C, A5, A7, A9 and A21 defect types are investigated in this graph. Based on the graph, as the density of vacancies goes up, the normalized critical buckling load reduces. The relationship is almost linear and the most drop is related to A21 configuration with approximately 12% reduction with respect to SLGS.

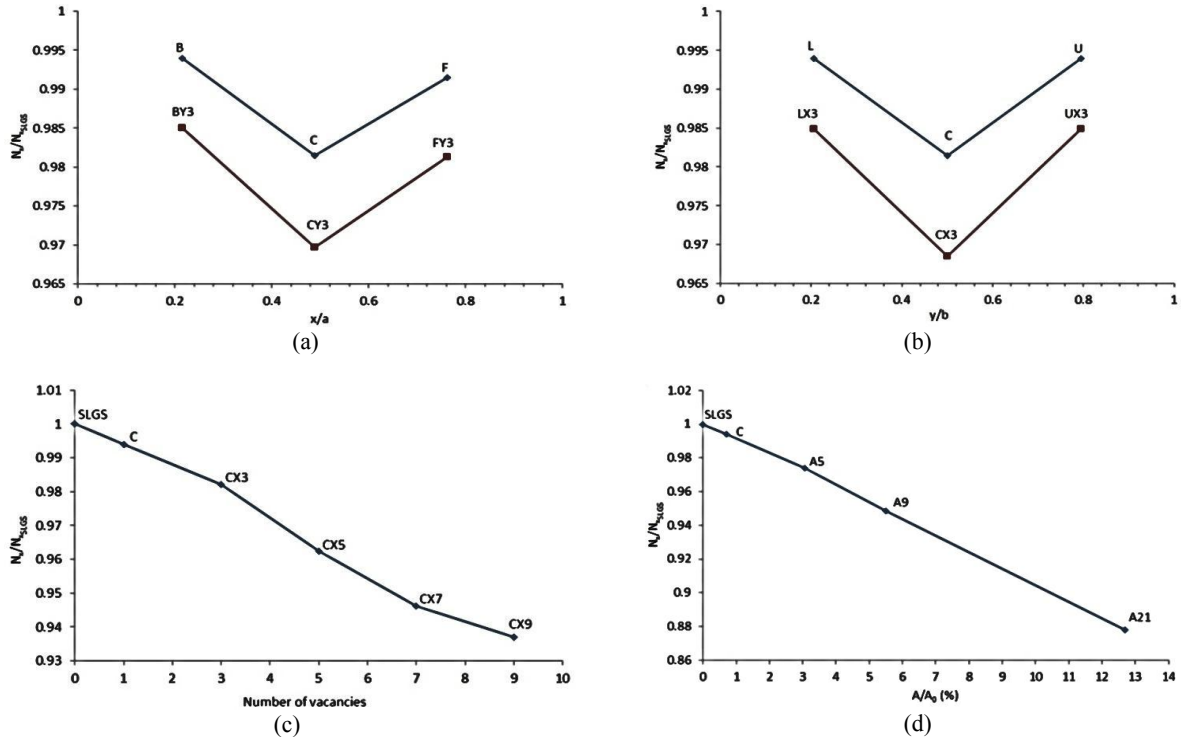

Fig. 9
Normalized critical buckling load, (a) Effect of vacancies in horizontal direction, (b) Effect of vacancies in vertical direction, (c) Effect of the number of vacancies in horizontal direction, (d) Effect of areal density of vacancies.

8 CONCLUSIONS

A valid finite element analysis of a single layer graphene nanosheet using structural mechanics approach was presented. On the base of this model, the effect of vacancy location, number and density of defects on the critical buckling load of a simply supported rectangular single layer graphene nanosheet have been investigated. On contrary to the Young's modulus, which the vacancy location has negligible effect in its value, the uniaxial buckling load shows considerable variation when the position of a vacancy defect changes. Also an upward trend in the number of vacancies leads to an approximately linear decline in the value of critical buckling load.

REFERENCES

[1] Sakhae-pour A., Ahmadian M.T., Naghdabadi R., 2008, Vibrational analysis of single-layered graphene sheets, *Nanotechnology* **19**: 085702.

[2] Li C.Y., Chou T.W., 2004, Mass detection using carbon nanotube-based nanomechanical resonators, *Applied Physics Letters* **84**: 5246.

[3] Sakhaee-Pour A., Ahmadian M.T., Vafai A., 2008, Applications of single-layered graphene sheets as mass sensors and atomistic dust detectors, *Solid State Communications* **145**: 168-172.

[4] Dai H., Hafner J. H., Rinzler A. G., Colbert D. T., 1996, Nanotubes as nanoprobes in scanning probe microscopy, *Nature* **384**: 147-150.

[5] Pradhan S.C., Murmu T., 2010, Small scale effect on the buckling analysis of single-layered graphene sheet embedded in an elastic medium based on nonlocal plate theory, *Physica E* **42**: 1293-1301.

[6] Tapia A., Peon-Escalante R., Villanueva C., Aviles F., 2012, Influence of vacancies on the elastic properties of a graphene sheet, *Computational Materials Science* **55**: 255-262.

[7] Lu Q., Huang R., 2009, Nonlinear mechanics of single-atomic-layer graphene sheets, *International Journal of Applied Mechanics* **1**(3): 443-467.

[8] Rapaport D.C., 2004, *The Art and Science of Molecular Dynamics Simulation*, Cambridge University Press, Cambridge.

[9] Frenkel D., Smit B., 2002, *Understanding Molecular Simulation: From Algorithms to Applications*, Academic Press, San Diego.

[10] Hu H., Onyebueke L., Abatan A., 2010, Characterizing and modeling mechanical properties of nanocomposites-review and evaluation, *Journal of Minerals and Materials Characterization and Engineering* **9**(4): 275-319.

[11] Li C., Chou T.W.A., 2003, A structural mechanics approach for the analysis of carbon nanotubes, *International Journal of Solids and Structures* **40**: 2487-2499.

[12] Sakharova N.A., Pereira A.F.G., Antunes J.M., Fernandes J.V., 2016, Numerical simulation study of the elastic properties of single-walled carbon nanotubes containing vacancy defects, *Composites Part B* **89**: 155-168.

[13] Canadijal M., Brcicl M., Brnicl J., 2013, Bending behavior of single layered graphene nanosheets with vacancy defects, *Engineering Review* **33**(1): 9-14.

[14] Hemmasizadeh A., Mahzoon M., Hadi E., Khandan R., 2008, A method for developing the equivalent continuum model of a single layer graphene sheet, *Thin Solid Films* **516**: 7636-7640.

[15] Shokrieh M.M., Rafiee R., 2010, Prediction of Young's modulus of graphene sheets and carbon nanotubes using nanoscale continuum mechanics approach, *Materials and Design* **31**: 790-795.

[16] Cheng Y.Z., Shi G.Y., 2014, Equivalent mechanical properties of graphene predicted by an improved molecular structural mechanics model, *Key Engineering Materials* **609-610**: 351-356.

[17] Boukhvalov D.W., Katsnelson M.I., 2008, Chemical functionalization of graphene with defects, *Nano Letters* **8**: 4373-4379.

[18] Zhang X., Jiao K., Sharma P., Yakobson B., 2006, An atomistic and non-classical continuum field theoretic perspective of elastic interactions between defects (force dipoles) of various symmetries and application to graphene, *Journal of the Mechanics and Physics of Solids* **54**: 2304-2329.

[19] Lu P., Zhang P.Z., Guo W., 2009 ,Electronic and magnetic properties of zigzag edge graphenenanoribbons with Stone–Wales defects, *Physics Letters A* **373**: 3354-3358.

[20] Fan B., Yang X., Zhang R., 2010, Anisotropic mechanical properties and Stone-Wales defects in graphene monolayer: A theoretical study, *Physics Letters A* **374**: 2781-2784.

[21] Tsai J.L, Tzeng S.H., Tzou Y.J., 2010, Characterizing the fracture parameters of a graphene sheet using atomistic simulation and continuum mechanics, *International Journal of Solids and Structures* **47**: 503-509.

[22] Xiaoa J.R., Staniszewskia J., Gillespie Jr J.W., 2010, Tensile behaviors of graphene sheets and carbon nanotubes with multiple Stone–Wales defects, *Materials Science and Engineering: A* **527**: 715-723.

[23] Gelin B.R., 1994, *Molecular Modeling of Polymer Structures and Properties*, Hanser/Gardner Publishers, Cincinnati.

[24] Kalamkarov A.L., Georgiades A.V., Rokkam S.K., Veedu V.P., Ghasemi-Nejhad M.N. , 2006, Analytical and numerical techniques to predict carbon nanotubes properties, *International Journal of Solids and Structures* **43**: 6832-

6854.
[25] Allinger N.L., Yuh Y.H., Lii J.H., 1989, Molecular mechanics, the MM3 force field for hydrocarbons, *Journal of the American Chemical Society* **111**: 8551-8566.
[26] Cornell W.D., Cieplak P., Bayly C.I., 1995, A second generation force-field for the simulation of proteins, nucleic-acids, and organic molecules, *Journal of the American Chemical Society* **117**: 5179-5197.
[27] Sakhaee-pour A., 2009, Elastic properties of single-layered graphene sheet, *Solid State Communications* **149**: 91-95.
[28] Lier G.V., Alsenoy C.V., Doren V.V., Geerlings P., 2000, Ab initio study of the elastic properties of single-walled carbon nanotubes and graphene, *Chemical Physics Letters* **326**: 181-185.
[29] Kudin K.N., Scuseria G.E., Yakobson B.I., 2000, C2F, BN, and C nanoshell elasticity from ab initio computations, *Physical Review B* **64**: 1-10.
[30] Xiao J.R., Gama B.A., Gillespie Jr J.W., 2005, An analytical molecular structural mechanics model for the mechanical properties of carbon nanotubes, *International Journal of Solids and Structures* **42**: 3075-3092.
[31] Reddy C.D., Rajendran S., Liew K.M., 2005, Equivalent continuum modeling of graphene sheets, *International Journal of Nanoscience* **4**: 631-636.
[32] Wu Y., Zhang X., Leung A.Y.T., Zhong W., 2006, An energy-equivalent model on studying the mechanical properties of single-walled carbon nanotubes, *Thin-walled structures* **44**: 667-676.
[33] Natsuki T., Tantrakarn K., Endo M., 2004, Prediction of elastic properties for single walled carbon nanotubes, *Carbon* **42**: 39-45.
[34] Chen W.F., Lui E.M., 1987, *Structural Stability, Theory and Application*, Elsevier Science Publishing Co. Inc., New York.